An analytical stretching function that combines the best attributes of geopotential and terrain-following vertical coordinates

J.R. Siddorn*, R. Furner

Met Office, FitzRoy Road, Exeter EX1 3PB, United Kingdom

Abstract

This work provides a function for discretising the vertical coordinate in ocean models that is designed to allow the user to define a fixed surface resolution, as one can in geopotential coordinate models, whilst retaining the benefits of terrain-following coordinates. This formulation has been termed the γ stretching function and provides an analytical solution that, in contrast with hybrid schemes, allows gradual coordinate changes in the vertical and horizontal. The early part of the paper describes the theoretical framework in which this can be done. Following this a series of steps that are required to effectively implement the coordinate have been described, and a full description of the implementation for a shelf model, the Forecasting Ocean Assimilation Model (FOAM) Atlantic Margin Model (AMM7), is given. The FOAM AMM7 presently uses stretched terrain-following coordinates.

This implementation is then used to quantify the impact of the γ stretching compared with the current stretching scheme. This shows the new stretching to have improved slope and hydrostatic consistency parameters. As would therefore be expected the γ stretching is shown to give rise to reduced horizontal pressure gradient errors in an idealised seamount test case. The benefits of a constant and shallow box for air-sea exchange are demonstrated, with the γ stretching giving enhanced diurnal ranges, increased SSTs and shallower MLDs where the FOAM AMM7 is presently unable to well represent these properties.

Keywords:
oceanic boundary layer, vertical coordinates, modeling, shelf seas, NEMO, Atlantic, North-West European Shelf (NWS), North Sea, [48-60°N, -20-13°E], surface temperature

1. Introduction

Oceanic processes are either explicitly modelled or implicitly parameterised depending upon whether they are resolved by the model. This requires ocean model domains to be consistent with the natural length-scales of the ocean. If this is not the case then formulations and parameterisations can become ill-posed. These length-scales vary in both space and time, and one of the challenges for ocean modellers is to chose an appropriate grid spacing that allows the model scales to match those in the real world for the processes being modelled. If the model grid scales vary they should do so consistently with the natural scales of the ocean, otherwise the model solution becomes inconsistent. Although considerable effort is made to improve the way we formulate ocean processes in our models, when considering the impact upon the quality of ocean model simulations the choice of vertical coordinate is the single most important factor (Chassignet et al., 2000; Haidvogel and Beckmann, 1999; Griffies et al., 2000). This paper describes a novel method for defining ocean model vertical coordinates that is designed to improve this alignment of scales between the ocean model and the real ocean.

Ocean models can be discretized in the vertical using geopotential, terrain-following, isopycnal or pressure-coordinate systems. A useful description of vertical coordinates is available in Song and Hou (2006). The aim of this work is to improve simulations using the Nucleus for European Modelling of the Ocean model (NEMO; Madec, 2008) and will therefore only consider geopotential and terrain-following coordinates, with isopycnal and pressure coordinates not being available in the NEMO framework. In particular, the aim is to improve the Met Office short-range forecasting model of the North-West European Continental Shelf (NWS), the Forecasting Ocean Assimilation Model Atlantic Margin Model at approximately 7 km (the FOAM AMM7, Figure 1). A full description of the model is given in O'Dea et al. (2012). This is a three-dimensional baroclinic model using NEMO, that has stretched terrain-following coordinates based upon Song and Haidvogel (1994). It is nested into a geopotential coordinate eddy-resolving basin scale model of the North Atlantic, the FOAM NATL12 (Storkey et al., 2010).

Geopotential coordinates (commonly referred to as Z-coordinates) are the most commonly used vertical coor-

*Corresponding author
Email address: john.siddorn@metoffice.gov.uk (J.R. Siddorn)

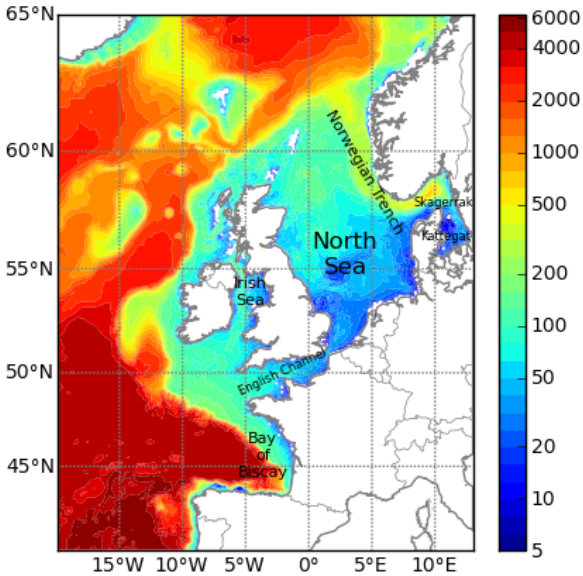

Figure 1: The bathymetry of the North-West European Continental Shelf (NWS), as used in the FOAM AMM7 model.

dinate system, at least for deep ocean applications. The vertical coordinate is discretized onto fixed levels that are taken as a depth from a reference level at or near the top of the water column (for example the mean sea level or, in non-linear free surface applications, the sea surface). The vertical levels normally have different thicknesses which allows the resolving of surface mixing and upper ocean dynamics without the computational overhead of a large number of vertical levels. However, this schema does not allow a good representation of varying topography because the bottom slope becomes approximated by a series of steps. This leads to inaccurate representation of the bottom boundary layer through poor representation of kinematic conditions (Gerdes, 1993) and bottom pressure torques (Bell, 1999; Hughes and de Cuevas, 2001; Song and Wright, 1998). This leads to problems when representing the flow between shallow and deep waters (Roberts and Wood, 1997; Beckmann and Döscher, 1997) and hence leads to the poor representation of flows over sills and ultimately deep water formation. This has been partially mitigated through the use of partial or shaved-cell techniques (Adcroft et al., 1997; Pacanowski and Gnanadesikan, 1998).

Terrain-following coordinates, introduced as a concept for meteorological modelling by Phillips (1957), transform real space into a dimensionless computational domain bounded by the sea surface on the one hand and the sea bed on the other. This coordinate type is generally referred to as a σ-coordinate when the domain is equally divided or S-coordinate if some stretching is applied. Terrain-following coordinates are most commonly used in models that are predominantly designed for shelf or coastal applications, for example the Regional Ocean Modelling System (ROMS; Shchepetkin and McWilliams, 2005) and the Proudman Oceanographic Laboratory Coastal-Ocean Modelling System (POLCOMS; Holt and James, 2001) and have also been implemented in the NEMO model to allow its use for coastal applications. The major advantage of this system is that it follows the topography, and therefore naturally represents the bottom boundary conditions. However, as the coordinate is defined in computational space rather than real space it is not independent of local depth, and thus in applications where the topography being modelled varies significantly then so does the vertical resolution. Another significant downside with σ/S-coordinates is their use results in errors in the calculation of the horizontal pressure gradient, particularly over steep topography (Janjić, 1989; Haney, 1991). Recent advances in the calculation of horizontal pressure gradients (e.g. Shchepetkin and McWilliams, 2003) however have reduced these errors. The horizontal pressure force in σ/S-coordinates consists of two terms, the pressure force along the model coordinate and a correction term that depends on both the tilt of the coordinate surface relative to the horizontal and the rate of change of the pressure in the vertical. This introduces an error that is a function of the S-coordinate slope and the stratification as well as model resolution, the equation of state, the form of the horizontal pressure gradient calculation and the finite difference scheme (Haney, 1991; Beckmann and Haidvogel, 1993). Other errors are also introduced when using sloping coordinates, due to what is often termed errors in hydrostatic consistency, whereby adjacent grid cells in coordinate space are not well aligned in real space.

A terrain-following coordinate, therefore, that minimises the coordinate slope, especially near regions of high stratification, would be expected to minimise computational errors. Similarly, a coordinate system that allowed enhanced resolution near areas of dynamic variability would allow these dynamic processes to be better resolved. For this reason stretching is applied. Atmosphere models have for many years used terrain-following coordinates, and there are a number of methods for stretching the coordinate. Schär et al. (2002), for example, developed a function that removes high frequency variability in the topography from the coordinate and hence significantly reduces numerical truncation errors. However, the ocean is fundamentally different to the atmosphere in that the range of depths in the ocean are the same as, or at least of the order of, the maximum depth (i.e. the depth of the water goes to zero) whereas in the atmosphere the variability in the orography is only a small proportion of the total modelled depth. This makes the stretching functions used in atmosphere models generally unsuited to use in oceans. Stretching functions have therefore been developed for ocean modelling, for example those of Madec et al. (1996) or Song and Haidvogel (1994) which are presently available within the NEMO frame-

work. Mixed terrain-following and geopotential coordinates have also been used, for example Mellor et al. (2002) and Gerdes (1993) (on which the NEMO formulation used by Madec et al. (1996) is based). However, these mixed coordinate systems do not have smooth analytical solutions and thus have a tendency to generate large changes in vertical resolution, which is not numerically satisfactory. Alternatively, σ/S-coordinates have been adapted to vanish through the sea bed in what Dukhovskoy et al. (2009) refer to as Vanishing Quasi-Sigma (VQS) coordinates. These coordinates, available within NEMO, allow the σ-coordinate to follow a pseudo-bathymetry below the real bathymetry at times when the bottom slope becomes steep, reducing the coordinate slope and thus the pressure-gradients. This can be helpful, but in effect reverts the model to a stepped bathymetry in some regions and so reduces the benefit of having a terrain-following coordinate with regards to the bottom stress calculations.

Decisions on which coordinate system to use depend upon the application for which the model is intended. Applications on or including shelf waters tend to use S-coordinates to allow the interaction with the relatively shallow bottom to be well resolved. These coordinates give variable resolution at the surface leading to inconsistencies in the simulation of surface processes across the domain. The importance of this is obvious if using the ocean model for providing predictions of surface temperature or currents. It is also important in a coupled ocean-atmosphere system to provide realistic boundary layer conditions of temperature and momentum to the atmosphere and in providing well-prescribed air-sea exchange of gases in an Earth System Model. The AMM7 is a shelf-wide model that spans depths from 10 m in coastal areas to 300 m across the shelf-break and into the deep ocean at greater than 5000 m (Figure 1). The surface grid box depth in this model ranges over three orders of magnitude, resolving diurnal cycles in some parts of the domain and not in others. This means it does not optimally resolve the surface properties, and is not well suited to use as part of a coupled system. It also means that interpretation of the model solutions in the near surface is often difficult.

This is simply resolved by switching to using a Z-coordinate model, where the surface grid box depth is prescribed and, given sufficient numbers of vertical levels to allow a reasonable gradient in the cell depths, can be set to whatever the modeller deems fit. A sensible surface depth can be then be prescribed to explicitly resolve some processes (diurnal layers, wind driven surface flows) and allow for sub-grid scale parameterisation for others (i.e. heat exchange at the viscous scale, surface wave breaking). However, given the disadvantages of using Z-coordinates in the AMM region a better option would be to design a stretching function that allows terrain-following coordinates to emulate the fixed surface of Z-coordinates. A number of schemes have been used that mix terrain-following and geopotential coordinates. These, however, have the disadvantage of not being pure analytical functions and thus do not provide a smooth solution.

This paper outlines an analytically derived, and thus smooth, vertical coordinate system that is terrain-following and allows a constant surface and/or bottom grid box depth.

2. Methods

2.1. Defining the vertical coordinate

The vertical coordinate is defined in computational space such that:

$$z = \gamma\,(H + \zeta) \quad \text{with} \quad 0 \leq \gamma \leq 1 \tag{1}$$

where z is the geopotential depth (positive downwards from the sea surface), H is the total water depth and ζ is the free surface. γ is a function (derived below) of σ, and σ defines the unstretched coordinate space, indexed in the integer k from 0 to $n-1$ to give n surfaces:

$$\sigma = \frac{k}{n-1} \quad \text{where} \quad 0 \leq k \leq n-1 \tag{2}$$

The function γ is derived so that it meets the following constraints:

- the surface cell depth (Z_s) and bottom cell depth (Z_b) are user prescribed as real depths and included in the analytical function
- the function allows user controlled stretching at the surface and bottom
- the function contains a dependant variable that adapts the grid to allow the integral to be constrained to one
- the function is constrained to a montonically increasing solution
- the rate of change of cell depths in both the horizontal and the vertical is minimised to reduce noise

It is also desirable for the coordinate to converge on σ or Z-coordinates in shallow water.

A number of formulations were explored, for example based upon Song and Haidvogel (1994) and Pietrzak et al. (2002) coordinates, but were found to be unable to give a reasonable analytical profile when the above constraints are applied over a wide range of depths. A constrained solution based upon the Song and Haidvogel (1994) formulation worked reasonably for a depth range of a few hundred metres, but requires a prohibitive number of vertical levels to work of larger depth ranges. A formulation found to have suitable characteristics is given below. A number of other formulations may well be suitable and could be derived using similar methodologies.

2.2. The analytical solution

The solution for γ is derived by defining the differential of the stretched coordinate system. The function is formed of three parts. One is a function of $(1-\sigma)$ and controls the stretch towards the surface. Another is a function of σ and controls the stretch towards the bottom. Additionally a function of $\sigma(1-\sigma)$ and a dependant variable (X) is included to give the function flexibility, enabling it to meet the imposed constraints. This incorporates a user controlled stretching parameter (α) to give some control over the functions shape. A number of variants on this functional form were explored, some of which could not be solved, gave overly complicated solutions or did not give adequate control over the function shape. After some trial and error the following form was found to be both mathematically solvable and effective.

$$\frac{d\gamma}{d\sigma} = A(1-\sigma) + 3B\sigma^2 + X(\alpha+1)(\alpha+2)\sigma^{\alpha}(1-\sigma) \quad (3)$$

Given the constraints at the surface, $\gamma = 0$ when $\sigma = 0$, and the bottom, $\gamma = 1$ when $\sigma = 1$, this can be integrated and solved for X, giving:

$$\gamma = A\left(\sigma - \frac{1}{2}\left(\sigma^2 + f(\sigma)\right)\right) + B\left(\sigma^3 - f(\sigma)\right) + f(\sigma) \quad (4)$$

Where:

$$f(\sigma) = (\alpha+2)\sigma^{\alpha+1} - (\alpha+1)\sigma^{\alpha+2}$$

The solution can be constrained to given specified surface (Z_s) and bottom (Z_b) grid cell depths, as σ has known solutions at all values of k, and prescribing the surface and bottom cell depths also therefore constrains γ at $k=1$ and $k=n-2$:

$$\gamma\big|_1 = \frac{Z_s}{H+\zeta} \qquad \gamma\big|_{n-2} = 1 - \frac{Z_b}{H+\zeta}$$
$$\sigma\big|_1 = \frac{1}{n-1} \qquad \sigma\big|_{n-2} = 1 - \frac{1}{n-1}$$

For a time invariant solution ζ can be assumed to be zero. In a non-linear free surface model this will result in differences in the grid resolution as the free surface varies which must be taken into account. The impact is normally small and so for most applications the coordinate may be calculated once, with ζ taken to be zero, and remain fixed (in computational space) throughout the simulation. For the remainder of this work the coordinate is calculated in this way, and so it should be noted that the actual grid resolutions (following Equation 1) vary in time as a function of ζ. It would, if desired, be straightforward to substitute $H+\zeta$ for H into Equations 5 and 6 and recalculate the coordinate in computational space at every timestep to give an exact solution for the surface and bottom grid cell resolutions in real space.

Substituting for these into Equation 4 allows a unique solution to be found for A and B:

$$A = \frac{1 - \frac{Z_b}{H} - \lambda_3\left(\frac{Z_s}{H} - \lambda_1\right) - \lambda_2}{n_2 - \frac{1}{2}\left(n_2^2 + \lambda_2\right) - \lambda_3\left(n_1 - \frac{1}{2}\left(n_1^2 + \lambda_1\right)\right)} \quad (5)$$

$$B = \frac{\frac{Z_s}{H} - \lambda_1 - A\left(n_1 - \frac{1}{2}\left(n_1^2 + \lambda_1\right)\right)}{n_1^3 - \lambda_1} \quad (6)$$

Where:

$$n_1 = \frac{1}{n-1}$$
$$n_2 = 1 - \frac{1}{n-1}$$
$$\lambda_1 = (\alpha+2)n_1^{\alpha+1} - (\alpha+1)n_1^{\alpha+2}$$
$$\lambda_2 = (\alpha+2)n_2^{\alpha+1} - (\alpha+1)n_2^{\alpha+2}$$
$$\lambda_3 = \frac{n_2^3 - \lambda_2}{n_1^3 - \lambda_1}$$

The water depth at the coordinate surface is now fully described with Equations 1, 2 and 4 in terms of the user-prescribed parameters, Z_s, Z_b, α and n and the water depth, H.

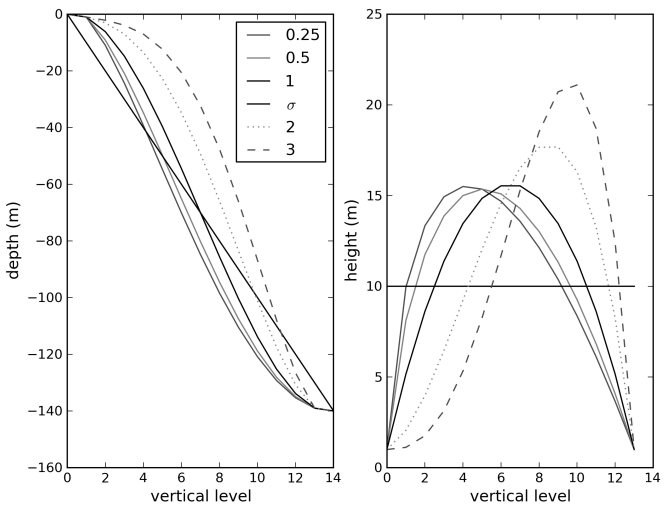

Figure 2: The change in the vertical coordinate with change in α. Shown on the left is the depth of the coordinate in a 140 m water column where 15 levels are used, and on the right is the corresponding cell height. Surface and bottom cell resolutions are fixed at 1 m for all cases expect that labelled σ, which has Z_s and Z_b set at 10 m ($\frac{1}{n-1}$). The values used for α are shown in the figure legend, except for the σ case where it is 1.0.

One of the potential criticisms of any vertical coordinate solution that is heavily constrained would be that the user control of the coordinate is potentially reduced. That would appear at first glance to be the case in the γ coordinate. However it turns out to have a very convenient

property. The extent and position of the stretching are a function of α such that if α is unity, there is no stretching except that required by the definitions of Z_s and Z_b, if it is less than unity the coordinate gives greater resolution in the surface and less towards the bottom, and vice versa if greater than unity. This allows the user to recreate pure σ-coordinates in the special case where Z_s and Z_b are both equal to $\frac{H}{n-1}$. Figure 2 shows the impact of changing α in the case where Z_s and Z_b are equal, and in the case where additionally both are equal to $\frac{H}{n-1}$, and shows the stretching towards the surface for $\alpha > 1$ and towards the bottom for $\alpha < 1$.

The γ function described here will work in waters of all depths, although may produce undesirable stretching if not applied carefully. The following section describes how to constrain the coordinate solution so that it can be used in practice.

2.3. Constraining the solution

2.3.1. Shallow water

In shallow water, where the prescribed surface and bottom depths become large relative to $\frac{H}{n}$, the stretching will result in a coordinate that increases in resolution away from the surface/seabed. It is therefore desirable that in water depths shallower than some critical depth H_c the coordinate is treated differently to prevent this. Two options are considered, the coordinate transitioning to σ-coordinates or to Z-coordinates. This is simply done by applying the following transformation at depths less than the critical depth (H_c):

$$z\big|_{H<H_c} = \begin{cases} \sigma H & \text{for } \sigma \text{ coordinates} \\ \sigma H_c & \text{for } Z\text{-coordinates} \end{cases} \tag{7}$$

The Z-coordinate form requires the vertical coordinate system to be able to deal with inactive cells in a stretched coordinate framework; NEMO for example allows this and this functionality is already used in short-range shelf applications at the Met Office. The advantage of the latter (pseudo Z-coordinate) over the σ approach is that it keeps a prescribed surface/bottom resolution, although has the disadvantages at the seabed described previously. Chosing a σ-coordinate in the shallow water will allow improved model solutions at the expense of increasing the resolution at the surface and hence potentially creating inconsistent air-sea exchange.

To ensure a gradual transition from the shallow to deep formulations H_c should be approximately $n\left[\frac{Z_s+Z_b}{2}\right]$. To prevent sharp changes in the coordinate smoothing must be applied around H_c, as a function of $H - H_c$. This is achieved by stipulating that for $H \geq H_c$:

$$z = \gamma H \left[\tanh\left(\frac{H-H_c}{e}\right)\right] + \sigma H \left[1 - \tanh\left(\frac{H-H_c}{e}\right)\right] \tag{8}$$

where e is a transition length scale. It is worth noting that the vertical coordinate will differ from the prescribed surface and bottom resolutions close to H_c, and the extent to which it does so depends on the length scale e and the change in Z_s/Z_b at H_c.

2.3.2. Deep waters

In waters of depth greater than the critical depth, H_c, the analytical solution described in Equations 4 and 8 are used. These satisfy many, but not all, of the criteria for the coordinate system. The solution does not give a monotonically increasing value of γ in all cases. Nor does it always give a gradually varying grid cell size in either the vertical or horizontal dimensions.

To ensure a monotonically increasing solution the following must be true.

$$\gamma_{k+1} - \gamma_k > 0 \tag{9}$$

Similarly, for the solution to be gradually increasing in the vertical, to a given tolerance (χ), the following must also be true:

$$\left|\frac{\gamma_{k+1} - \gamma_k}{\gamma_k - \gamma_{k-1}} - 1\right| < \chi \tag{10}$$

A tolerance of approximately 30 %, or $\chi = 0.3$ gives vertical changes in grid size of a similar order to those used presently in the Met Office Z-coordinate and S-coordinate models. The smaller the value of χ chosen (strong constraint) the slower the vertical coordinate can change, and hence the more limited the coordinate becomes. The larger χ (weak constraint) the greater the range of depths that can be chosen for the surface and bottom box, but with the increased rate of change of the coordinate comes increased risk of numerical artefacts.

The above criteria are not straightforward to apply analytically, but can be used to define the range of acceptible input values for the user controlled parameters. In practice the value for n will be limited by the computational cost of the solution and for most applications Z_s will be expected to be constant to ensure consistent representation of air-sea exchange processes. Once n and Z_s have been chosen, it is therefore neccessary to explore the acceptable parameter ranges for Z_b and α, given the constraints on monotonicity and rates of change given in Equations 9 and 10. Selecting Z_b and α within these ranges leaves all criteria met except the stipulation that the stretching minimises the rate of change of the coordinate for adjacent cells in the horizontal. The variations between heights of adjacent grid cells is determined by a combination of the stretching and the variation in the bathymetry. The shape of the stretching function, and its intensity, determine how much of an impact this will have. It is possible to create a coordinate with undesirable oscillations in the horizontal coordinate which are unrelated to changes in the bathymetry. These are caused by changes in the user

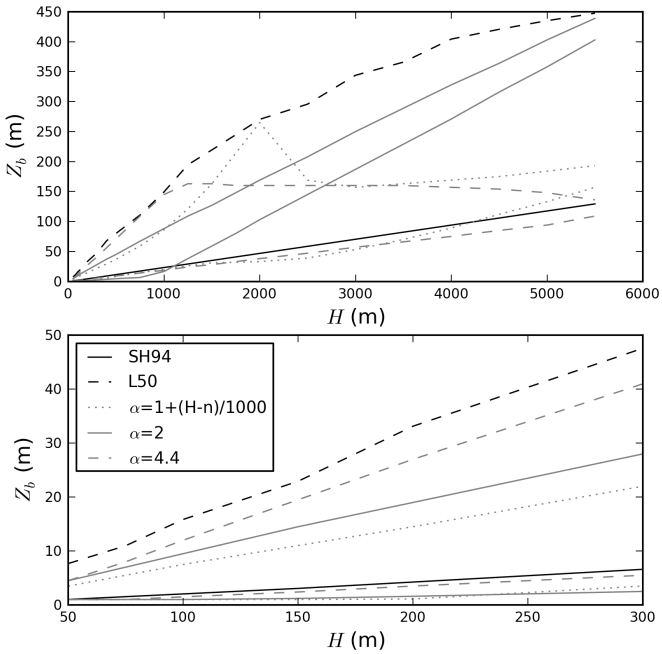

Figure 3: Depth of the bottom cell, Z_b, for a given total water depth, H, for a Song and Haidvogel (1994) stretch coordinate (SH94, dashed line), a Z-coordinate (L50, solid line) and three different γ stretching sets (grey lines). For the γ stretching the minimum and maximum possible Z_b for a χ of 0.3, Z_s of $1.0m$ and different values for α (see legend) is shown. All coordinates use 50 vertical levels. The plot on the top shows the full range of depths tested, and the bottom plot only shelf-slope depths

defined variables and so can be prevented by ensuring that Z_s, Z_b and α either remain constant or vary gradually as a function of bathymetric depth. Some experimentation of the sensitivity to these parameters for a new configuration would be needed and the resultant coordinate should be carefully checked.

An example of the sensitivity to the choice of values for α and Z_b has been explored in an idealised case where the bathymetry ranges from 50 m to 5500 m (Figure 3). The number of vertical cells used is 50 and the surface resolution (Z_s) is 1 m. The figure compares the depth of the bottom grid cell (Z_b) for three coordinates, a geopotential coordinate used in FOAM for deep ocean modelling that has a 1 m surface resolution and 50 vertical levels (labelled L50), a terrain-following coordinate based upon Song and Haidvogel (1994) stretching as used in the AMM7 model (labelled SH94; for comparability this example uses 50 levels rather than the 34 used by the AMM7) and the γ stretching with three different prescribed values for α. The maximum and minimum possible values for Z_b in the γ coordinate given $n = 50$, a surface resolution of 1 m ($Z_s = 1.0$), stipulation of monotonicity (as given in Equation 9) and a χ of 0.3 (Equation 10) are shown giving the envelop of acceptable values for Z_b given the prescribed Z_s and α values.

The choice of α determines the ranges of Z_b that are allowable given the constraints applied and vice versa (Figure 3). It is notable that in this case no one value of Z_b can be used across all depths, which is not surpising given Z_s is relatively small and fixed, and there is a large range of depths being tested. Z_b would have to therefore vary as a function of water depth; it has already been noted above that it is desirable to introduce as little heterogeneity into the parameter space as possible. If the use of a constant value for α does not give desirable stretching then one would question whether the number of vertical levels is sufficient, or whether the surface grid resolution should be relaxed. Given the input parameters prescribed above, although the spatially varying α gives some benefits over the other solutions, it is actually rather similar to the $\alpha = 5$ solution, and therefore setting a constant α would be sensible in this case.

In Figure 3 the ranges of the bottom resolution allowable can be described as L50-like with $\alpha = 2$ and SH94-like with $\alpha = 4.4$. They both allow high resolution at the bottom in shallow water and down to the bottom of the shelf slope. The key difference is the SH94-like option keeps the resolution relatively high at the bottom, mimicking the SH94 solution in deep water, whereas the L50-like solution transitions to give a solution similar to the FOAM L50 model in deep water.

3. Results

3.1. The stretched coordinate for a shelf application

The primary motivator for this work is to improve the vertical coordinate in a tidal model, the AMM7 (O'Dea et al., 2012), that covers a region of the ocean that includes deep water in the North Atlantic and in the Norwegian Trench but is primarily run to produce forecasts for the wide, shallow European North-West Shelf itself. Traditional Z-coordinate systems have inherent weaknesses for this and similar domains, namely that Z-coordinates require a large number of vertical coordinates to adequately resolve all waters, and the bottom boundary condition is poorly represented, and so σ/S-coordinates are generally used. However these are unable to give a consistent and high resolution surface coordinate. The AMM7 uses an S-coordinate following Song and Haidvogel (1994). Recent extensive evaluation of the AMM7 show the Sea Surface Temperature (SST), and diurnal signals in it, are poorly represented in deep water. The poor resolution of the surface can be clearly seen in SST fields from the AMM7 when compared with those from the Z-coordinate FOAM model into which it is nested. This is an issue as SST is an important product from the AMM7 in its own right, and looking forward to a future Numerical Weather Prediction system that includes ocean-atmosphere coupling, a poor representation of SST (and to a lesser extent surface currents) will limit the utility of the coupled system.

Another known issue with the AMM7 is that water masses coming from the shallow Skagerrak/Kategatt region are not well resolved where they flow from the shallow regions of the southern Kattegat, into the considerably

deeper waters of the Skagerrak and on into the Norwegian Trench. This impacts upon the stratification in the Norwegian Trench and has both a local effect on the quality of temperature and salinity forecasts and an indirect impact on the quality of the simulations in the adjacent North Sea. The γ stretching is therefore in this example primarily proposed to maintain surface and near-surface resolution across a wide range of depths whilst maintaining the terrain-following bottom box.

The methodology described in Sections 2.2 and 2.3 above has been used to create a γ stretching for use in the AMM7 model. The choice of surface resolution, as described above, is relatively straightforward as 1 m is, after Bernie et al. (2005), considered optimal and also matches the Z-coordinate models used in the Met Office and elsewhere. The number of vertical levels required to get a reasonable coordinate given the constraints of having a 1 m surface has been found to be a minimum of approximately 50. The three cases for different values of α shown in Figure 3 all have potentially useful properties. Simulations (not shown) with the L50-like bottom resolution indicate that the loss of resolution at the bottom is undesirable. The use of $\alpha = 4.4$, given the potential to have high resolution at the bottom and the surface, has been chosen as optimal for the AMM7. This allows the specification of Z_b to be prescribed within the limits allowable with a χ of 0.3 as a function of the local water depth. The parameters $n = 51$, $Z_s = 1$ and $H_c = 50$, and at H_c, $Z_b = 1$ so that the γ and σ solutions are equal at the critical depth. In this case Equation 8 is not neccessary, and an efold number (e) of zero is used. In shallow waters ($H < H_c$) it has been chosen to reverts to σ-coordinates, rather than the pseudo-Z-coordinate. To maintain the required resolution whilst maintaining a smooth coordinate the following linear function in water depth has been chosen for Z_b:

$$Z_b = 0.024H - 0.2 \quad \text{for} \quad H > H_c \tag{11}$$

This implementation of the coordinate gives bottom resolutions very similar to those found in the Song and Haidvogel (1994) coordinate, and is used for all the following experiments.

The resultant vertical coordinate for the presently used Song and Haidvogel (1994) stretch coordinate (SH94), the Z-coordinate from FOAM (L50) and the γ stretching have been calculated for an idealised bathymetry (Figure 4 and 5). This shows the γ stretching has achieved the primary aim of maintaining high, and constant, resolution at the surface whilst maintaining the relatively high resolution near the bottom in shallow and intermediate waters. The coordinate gives the same resolution near the surface as the FOAM L50, which is a significant improvement on the SH94 stretching. The impact on air-sea exchange of using the γ coordinate over the SH94 formulation is shown in Section 3.4. It also gives better resolution than the FOAM L50 throughout the watercolumn in shallow and intermediate depth water, and keeps similar bottom resolution to the SH94 throughout the domain. It should also be noted that both the SH94 and the γ stretching give sloped coordinates, and there are noticable changes in the slope at their respective critical depths (150 m and 50 m respectively). It is important to understand the potential impact of the sloping surfaces. Section 3.2 investigates this in more detail. An idealised test case is presented in Section 3.3 that investigates the impact of the sloping surfaces upon the horizontal pressure gradient.

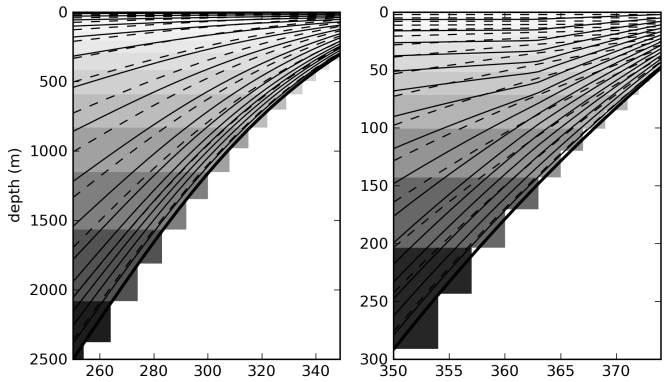

Figure 4: A comparison of the SH94 stretching (solid lines), the L50 Z-coordinate (contoured surfaces) and the γ stretching (dashed lines) for a idealised bathymetry. For clarity every third coordinate surface is shown. On the left shows waters from 500 m to 2500 m in depth and on the right from 50 m to 500 m.

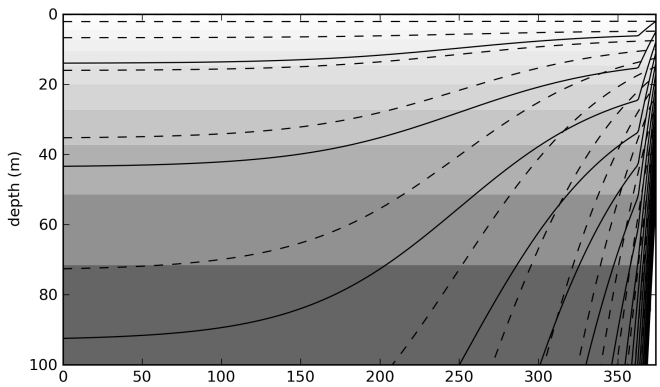

Figure 5: A comparison of the SH94 S-coordinate (solid lines), the L50 Z-coordinate (contoured surfaces) and the γ stretching (dashed lines) in the surface 100 m for a idealised bathymetry that goes from 50 m to 5500 m depth. For clarity every third coordinate surface is shown.

3.2. Quantifying the coordinate slope

Although stretching the coordinate be may desirable to generate increased resolution where it is required, this may come at the expense of increasing the slope of the coordinate and hence impacting upon the model's numerical accuracy. To understand this better a hydrostatic consistency parameter following Haney (1991) has been reformulated to deal with the stretched coordinate:

$$r = \frac{2}{S_k - S}\left|\frac{H_x}{H}S_x - S\right| \tag{12}$$

Where S denotes the coordinate in computational space, and could be the σ or SH94/γ stretched coordinate. The subscripts x, k denote values in adjacent grid cells to the side and below respectively, with the maximum of r for the four horizontal directions taken as the value of r for that point. An r of greater than unity formally violates hydrostatic consistency. It should be noted however that σ/S-coordinate models rarely meet this criteria. The aim is to therefore minimise the value of r, not to prevent the violation of hydrostatic consistency entirely.

A slope parameter, s, following Beckmann and Haidvogel (1993), but adapted for stretched terrain-following coordinates and therefore calculated at each depth level, is an alternative measure.

$$s = 2\left|\frac{HS - H_x S_x}{H + H_x}\right| \tag{13}$$

As with the hydrostatic consistency factor, the slope parameter is calculated in all horizontal directions, and the maximum slope used. This slope factor is a measure of the resolution compared to the bathymetric variability and its range is $0 < s < 1$, with values of zero when there is no slope (i.e. the resolution is infinite relative to the bathymetric variability) and is unity when the vertical change in depth for adjacent grid cells is the total water depth.

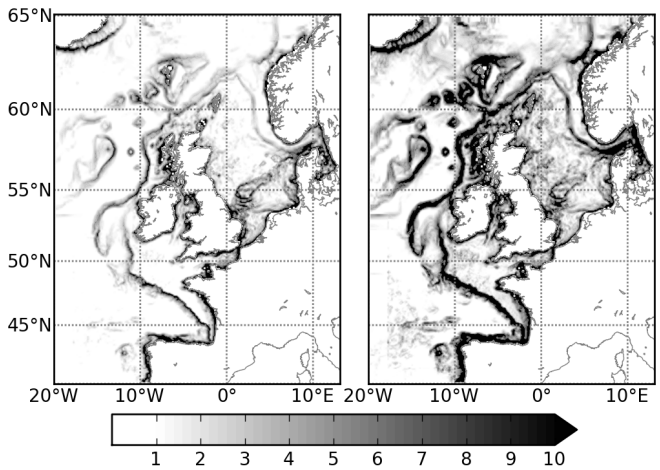

Figure 6: The depth mean hydrostatic consistency, r for the γ (left) and SH94 (right) stretching for the AMM7 domain with 50 levels.

The γ and SH94 stretching are compared using the slope factor (s) and hydrostatic consistency (r) on the AMM7 domain with 50 levels and on the seamount domain deescribed in 3.3. The γ stretching parameters used are described in Section 3.1 with the SH94 stretching using the parameter settings $\theta = 20$, $H_c = 150$ and $b = 0.8$, as used in the present AMM7 configuration. As these coordinates are stretched the values of r and s are a function of depth, and so for simplicity of interpretation the maximum and the mean over depth of both have been calculated. The maximima of both of these properties are generally found at the sea bed, and so in the case where the coordinate is matched at the bottom (as in this case) the maximimum is also very similar and so is not shown. Both the hydrostatic consistency and the slope parameter show similar results, with the γ stretching giving very considerably smaller values than the Song and Haidvogel (1994) setup. Both the slope factor and hydrostatic consistency increase up the slope of the sides of the seamount, reaching a maximum where the seamount flattens off (Figure 7). The difference in the coordinates is also clearly evident in the comparison on the AMM domain (Figure 6) with the γ stretching showing significantly smaller values over steep bathymetry (see Figure 1) such as along the shelf slope, around the Norwegian Trench, around the Faroe Isles and the Rockall Bank, where both the coordinate systems have maximum hydrostatic consistency and slope factors. The SH94 stretching also has significant areas on-shelf where the values are much higher than the γ stretching, due to its use of σ-coordinates in less than 150 m of water. In shallow waters (less than 50 m, for example in the southern North Sea) both stretching functions give the same (relatively high) values, as would be expected as both use σ-coordinates in these regions. This is encouraging and would indicate that this new coordinate should result in improved numerical accuracy. A demonstration of this improvement is given in 3.3.

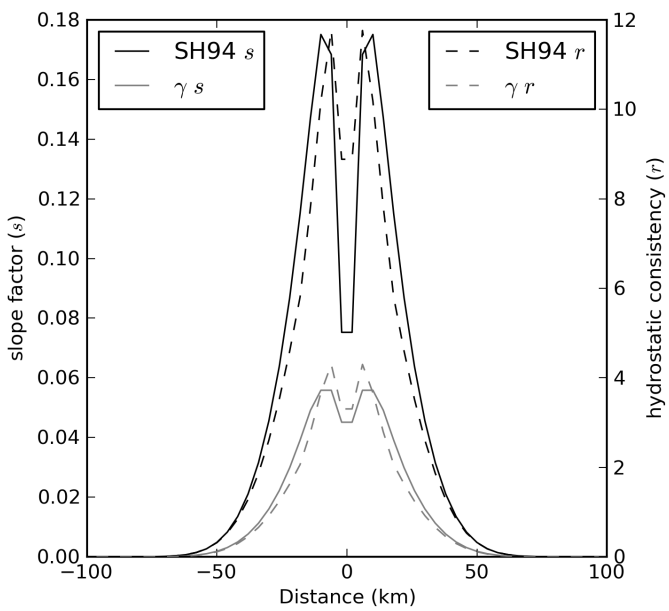

Figure 7: The depth mean hydrostatic consistency, r, and slope parameter, s, for the γ and SH94 stretching for an idealised seamount with 50 levels.

3.3. An idealised horizontal pressure gradient error test case

It has been hypothesised above that the γ stretching proposed in this paper, being flatter than the SH94 stretching near the surface and hence in regions of high stratification, should result in reduced horizontal pressure gradient errors.

An idealised experiment has been run with a seamount testcase very similar to that used by Beckmann and Haidvogel (1993) to test this hypothesis. No external forcing was applied to a mid-latitude (∼50°N) seasonally stratified ocean. No explicit horizontal or vertical diffusion was applied. Any velocities generated are therefore as a result (directly or indirectly) of the horizontal pressure gradient errors. The simulations were started from rest and initialised with a constant salinity profile, and a prescribed temperature profile of:

$$T_z = 5\left(1 - \tanh\left(\frac{z-120}{20}\right)\right) + 10\left(\frac{5500-z}{5500}\right)$$

Two simulations were run, one with the standard SH94 stretching of the AMM7 (although with the number of levels increased to 50) and the other with the γ stretching described in Section 3.1. Figure 8 shows the time evolution of the domain mean and maximum currents.

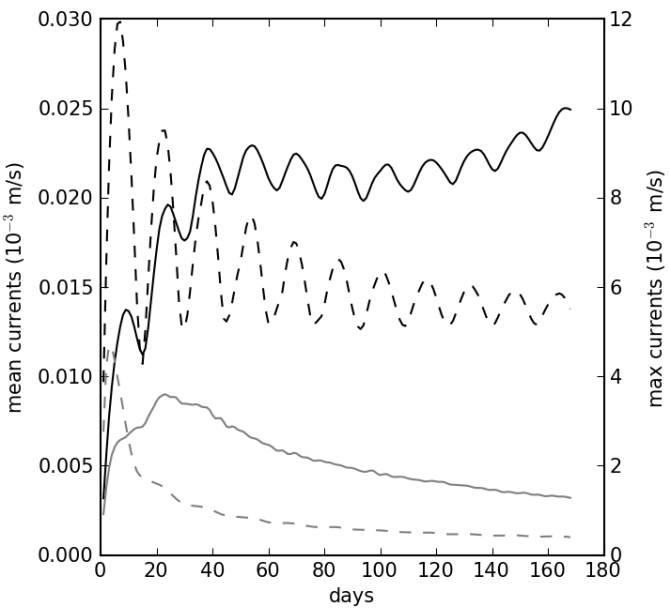

Figure 8: Current speeds (m/s) for a SH94 stretching (black) and γ stretching (grey). Domain mean currects for the domain are the solid lines, and domain maximum speeds are the broken lines. Both simulations started from rest, were initialised with an idealised stratification and had no applied forcing.

The Song and Haidvogel (1994) solution gives a very similar outcome to those presented in Beckmann and Haidvogel (1993), with domain maximum velocities spinning up quickly within 12 hours or less to give a domain maximum speed of 1 cm/s. These maxima oscillate over time at the inertial period of just under 16 hours, settling down to give a maximum speed of around 0.6 cm/s. The simulations using the γ stretching give quite different results, with the initial error being less than half that for the S-coordinate, and with insufficient velocities generated to sustain the oscillations. The γ simulation reaches a state where no oscillations occur and the maximum velocities are an order of magnitude smaller than for the SH94 simulation. This solution is a result of both the generally flatter coordinates with the γ stretching and the fact that the coordinates are most flat towards the surface, where maximum gradients in pressure occur.

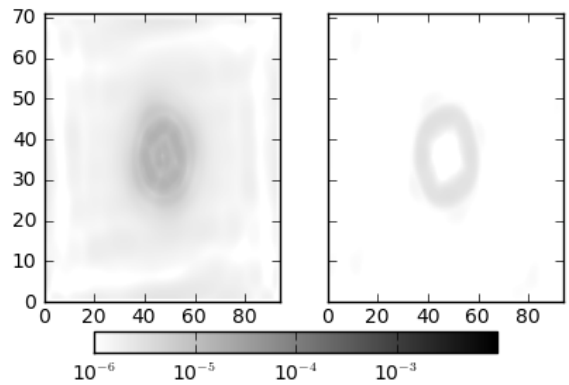

Figure 9: Depth mean current speeds (m/s) after 48 hours for the SH94 stretching (left) and γ stretching (right) from the same simulations as in Figure **??**.

Figure 9 shows the spatial pattern of the horizontal pressure gradient derived currents after 48 hours of simulation. This shows these erroneous currents closely follow the hydrostatic consistency parameter (see Figure 6) which in turn closely aligns to the gradients in bathymetry as is to be be expected. The change to the γ stretching does not qualititatively change the spatial distribution of these currents

3.4. An idealised air-sea exchange test case

To understand the potential impact of the change in the surface cell thickness on the AMM7 model in going from the SH94 to a γ formulation an idealised air-sea exchange test case has been run. The coordinates were implemented as described in Section 3.1 for the AMM7 model as described in O'Dea et al. (2012). The simulations were initialised with a surface temperature of 12°C and a tanh profile of temperature (below) similar to that used in the seamount testcase and that (given the temperature criterion detailed below) initialises the mixed layer to 80 m.

$$T_z = 3\left(1 - \tanh\left(\frac{z-120}{20}\right)\right) + 6\left(\frac{5500-z}{5500}\right)$$

The model was initialised with a constant salinity of 35.5 psu, and the simulations were run without boundaries, rivers or any external forcing other than prescribed heat fluxes to isolate the effects of the airsea exchange. A daily-averaged shortwave-radiation flux of 300 Wm^{-2}, with diurnal cycle, was imposed. A constant 400 Wm^{-2} of downward longwave-radiation was also imposed, and the radiative, sensible and evaporative heat fluxes were calculated using the CORE formulation (Large and Yeager, 2004) and a low, constant, background windspeed and a constant air temp of 16°C. This would be typical of warm, high-pressure periods in the early summer in the AMM7 area, and thus gives some indication of the model's response, in terms of forming a diurnal layer and modifying seasonal stratification.

To investigate the impact on stratification the daily maximum and minimum temperatures at each grid point for hourly instantaneous output was calculated. These maxima and minima were used to calculate a diurnal range. The mixed layer depth (MLD) at midnight was calculated using a simple temperature based criterion, where the mixed layer depth is taken to be the depth at which the temperature is 0.2° less than the SST.

After two days (Figure 10) the γ simulation has markedly shallower mixed layers, warmer nightime temperatures and a greater diurnal range than the SH94 simulation. This is most marked in the deeper waters but is still significant over the shelf slope and continental shelf regions. This is due to an improved representation of the ocean surface boundary layer in the γ stretching and the associated reduced implicit diffusion.

This is reflected in the regional mean evolution of the simulations (Figure 11). The figure shows waters for the on-shelf and shelf slope region (labelled shelf, and defined as waters of depths ranging from 50 m to 300 m) and for the deep waters (labelled offshelf, and defined as waters of depths greater than 300 m). Waters shallower than 50 m, where both coordinates are the same and significantly smaller differences occur, are not shown. In both simulations the mean diurnal range starts relatively large, decreasing as the mean temperature increases towards the air temperature. For the shallower waters the surface temperature increases more quickly, the mixed layer becomes more shallow and diurnal cycle is more pronounced than in the deeper waters, although the difference between the deep and shallower waters is less marked in the γ stretching simulation. This implies that vertical resolution is still a limiting factor in the deep waters for the new coordinate, but less so. Although the initial response of the simulations is quite different, they converge to similar solutions for diurnal range once the sea surface temperature approaches the air temperature (16°C). The mixed layer depth in the γ solution remains shallower in deep waters throughout the simulations, although the two simulations do appear to be slowly converging.

In summary, the γ stretching is more sensitive to surface heating, with a more rapid increase in surface temperatures, a more rapid and greater reduction in mixed layer depth and larger diurnal ranges. These impacts are to be expected given the change in the coordinate, and confirm the potential for the γ stretching to give better representation of the surface ocean both off shelf and on the shelf in regions with depths greater then 50 m.

4. Discussion

In this work the emphasis has been upon the use of the γ stretching in the AMM7, a model that presently uses terrain-following coordinates. The intention was to improve the representation of air-sea exchange in this model in deep waters, something that has been seen to be a weakness at present. It has been demonstrated that the γ stretching has the potential to improve the AMM7 in this way. It has also been shown that the hydrostatic consistency and slope factors are in general improved and the associated horizontal pressure gradient errors are reduced. Although it has not been demonstrated it is to be expected that, given the improved hydrostatic consistency and slope factor, other numerical artefacts will also be reduced.

Initially on commencing this work, the authors had envisaged running simulations of the AMM7 using realistic conditions and validating the results against observations. However, it became clear that the use of the γ stretching would not improve the AMM7 simulations immediately for two reasons. Firstly, the AMM7 is tuned (through bathymetric smoothing and bottom friction parameterisation) to have realistic shelf slope current and thus a realistic input of heat to the North Sea. It is clear that by reducing the horizontal pressure gradient errors, and therefore improving process representation, the simulations would no longer provide sufficient heat transport along the shelf slope current. Secondly, the AMM7 is known to have a tendency to be slightly warm at the surface, something that is thought to be due to a combination of the air-sea flux used and the downwelling radiation schemes. By improving the representation of heat-exchange at the surface the model would become warmer still, further increasing its bias.

It is intended that now the coordinate is well tested it will be implemented within the AMM7 as part of a suite of changes designed to improve the model.

Although the focus in this work has been upon the shelf seas models, where there is the need to model a wide range of water depths effectively, it has always been the intention of the authors that this coordinate should bridge the gap between deep ocean Z-coordinate and shelf seas σ-coordinate systems. As global ocean models become higher resolution there is an increasing potential for representing shallow water dynamics in deep ocean models. There is also a known problem in simulating flows over sills in global models. These flows are important in driving overturning circulations, and thus in determining global climate. It is therefore worth considering the potential for a terrain-following coordinate that gives a consis-

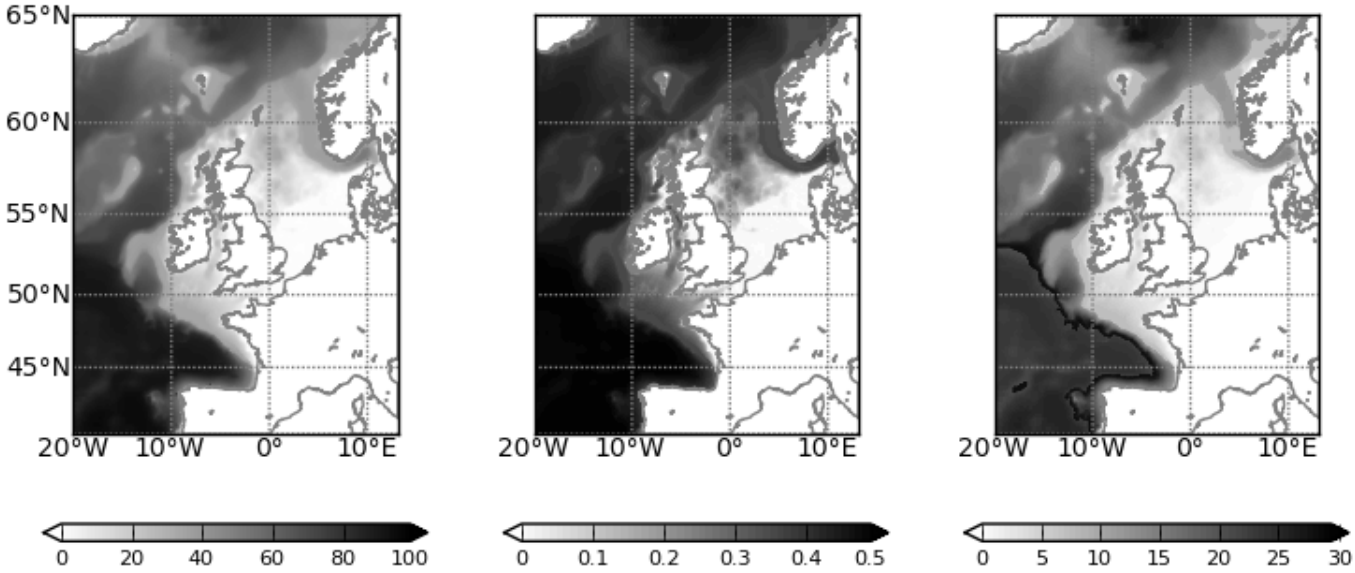

Figure 10: The difference between γ and SH94 stretching for diurnal range (%, left) midnight temperature (°C, middle) and midnight mixed layer depth (m, right). The difference in diurnal range is calculated as a proportion of the SH94 diurnal range. These are calculated so that a positive mixed layer depth difference means the γ stretching solution is shallower than the SH94, whereas positive diurnal ranges and midnight temperatures mean the γ solution is the larger.

tent representation of the surface and bottom boundaries in coupled ocean-atmosphere models of the climate.

Simulated Nordic Sea overflow entering into the deep North Atlantic through the Greenland-Iceland-Scotland (GIS) ridge is generally too weak in climate models with, for example, Met Office climate models giving GIS overflows of the order 3-4 Sv (Graham, pers comm), compared to the observed value of about 5-6 Sv from Dickson et al. (1990). This bias is thought to be caused by excessive convective entrainment of the overflow over staircase bathymetry in the model, leading to much lighter and shallower overflow waters (Winton et al., 1998). Danabasoglu et al. (2010) and other authors have attempted to correct these weak overflows with parameterisations that increase the overflows, with some partial success. Griffies et al. (2000) conclude that the ability to resolve these overflows is dependant upon the model vertical coordinate scheme, and that even with partial/shaved cells, Z-coordinate models do not capture these flows well. Ezer and Mellor (2004) compared the use of terrain-following and geopotential coordinate systems in modelling dense water overflows, and concluded that terrain-following coordinates could, at least in idealised case, provide realistic plume formation. It should also be noted that due to the smooth topography in terrain-following ocean models, they have the advantage of being stable with lower diffusivities than equivalent geopotential models (Mellor et al., 2002). This would suggest that climate modellers should be considering global model domains using terrain-following coordinates, if the disadvantages of poor representation of the surface exchange and high horizontal pressure gradient errors in terrain-following systems can be overcome.

A secondary benefit, therefore of this work, is expected to be the potential for improved water mass formation in climate prediction models. Historically, climate models have not used terrain-following coordinates, but recent work (Lemarié et al., 2012) suggests that this should be reconsidered given improved numerical solutions for terrain-following coordinates. A terrain-following coordinate that allows improved consistency in the surface grid resolutions over a range of water depths would further improve the potential for their use in climate simulations.

The Met Office Hadley Centre uses the NEMO model in its coupled ocean-atmosphere climate modelling system (HadGEM3; Hewitt et al. (2011)). The intention is to firstly look at the impact of the coordinate upon flows over sills and if it provides an improvement upon the present coordinates then to test it more generally within the coupled system.

The coordinate framework discussed here allows for the vertical grid spacings to adapt in time with the non-linear free surface through the inclusion of ζ in Equation 1 or to remain static in σ space (although not in real space) if ζ is not included. In general it is envisaged that the coordinate will not adapt in time due to the computational cost of recomputing it. However, the use the arbitrary lagrangian eulerian (ALE) method (Hirt et al., 1974) that has been implemented in NEMO (Leclair and Madec, 2011) could further reduce the spurious gradients at the coordinate surface.

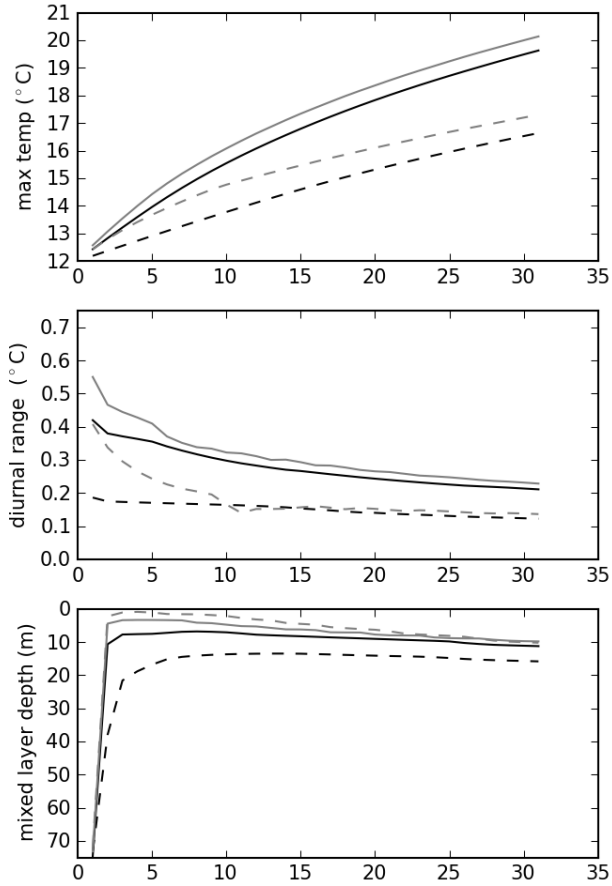

Figure 11: Comparison of mean daily maximum SST (top) mean diurnal range (middle) and mean mixed layer depth (bottom) for shelf (defined as 50 to 300 m depth waters; solid lines) and offshelf (greater than 300 m depth waters, dashed lines). The SH94 stretching simulation is in black and the γ stretching in grey.

5. Conclusions

The paper has defined a coordinate that can be shown, in theoretical cases at least, to be able to combine the representation of the ocean surface boundary layer in deep water associated with geopotential (Z) coordinate model frameworks with the ability of terrain (σ/S) coordinates to represent bottom boundary layers. It is also shown that the horizontal pressure gradient error associated with terrain-following coordinates is reduced using this coordinate as the mean slopes, and particularly the mean slopes in regions of high vertical density gradients, are less than a commonly used stretched coordinate.

This results in simulations that have fewer spurious currents due to numerical artefacts, and better representation of air-sea exchange, than the coordinate used presently for a stretched terrain-following coordinate model, the FOAM AMM7.

The potential for this coordinate to be used for global ocean models has not been explored here. It is expected that given advances in the numerics of terrain-following models, and the benefits they give for modelling flows over sills, that this work can be extended to coupled ocean applications with potential benefits for modelling overturning circulations.

Acknowledgements

Funding for this research is gratefully acknowledged from the Ministry of Defence, the Hadley Centre Climate Programme and from the European Community's Seventh Framework Programme FP7/2007-2013 under grant agreement 218812 (MyOcean). Helpful comments from Mike Bell on applying constraints to the mathematical solution are gratefully acknowledged. Advice on the model simulations from Enda O'Dea and from Gurvan Madec are also gratefully acknowledged.

References

Adcroft, A., Hill, C., Marshall, J., 1997. Representation of Topography by Shaved Cells in a Height Coordinate Ocean Model. Mon. Wea. Rev. 125, 2293–2315.

Beckmann, A., Döscher, R., 1997. A Method for Improved Representation of Dense Water Spreading over Topography in Geopotential-Coordinate Models. J. Phys. Oceanogr. 27, 581–591.

Beckmann, A., Haidvogel, D.B., 1993. Numerical Simulation of Flow around a Tall Isolated Seamount. Part I: Problem Formulation and Model Accuracy. J. Phys. Oceanogr. 23, 1736–1753.

Bell, M.J., 1999. Vortex stretching and bottom torques in the Bryan-Cox ocean circulation model. Journal of Geophysical Research 104, 23545–23563.

Bernie, D.J., Woolnough, S.J., Slingo, J.M., Guilyardi, E., 2005. Modeling Diurnal and Intraseasonal Variability of the Ocean Mixed Layer. J. Climate 18, 1190–1202.

Chassignet, E.P., Arango, H., Dietrich, D., Ezer, T., Ghil, M., Haidvogel, D.B., Ma, C.C., Mehra, A., Paiva, A.M., Sirkes, Z., 2000. DAMÉE-NAB: the base experiments. Dynamics of Atmospheres and Oceans 32, 155–183.

Danabasoglu, G., Large, W.G., Briegleb, B.P., 2010. Climate impacts of parameterized Nordic Sea overflows. Journal of Geophysical Research 115, C11005+.

Dickson, R.R., Gmitrowicz, E.M., Watson, A.J., 1990. Deep-water renewal in the northern North Atlantic. Nature 344, 848–850.

Dukhovskoy, D.S., Morey, S.L., Martin, P.J., O'Brien, J.J., Cooper, C., 2009. Application of a vanishing, quasi-sigma, vertical coordinate for simulation of high-speed, deep currents over the Sigsbee Escarpment in the Gulf of Mexico. Ocean Modelling 28, 250–265.

Ezer, T., Mellor, G.L., 2004. A generalized coordinate ocean model and a comparison of the bottom boundary layer dynamics in terrain-following and in z-level grids. Ocean Modelling 6, 379–403.

Gerdes, R., 1993. A Primitive Equation Ocean Circulation Model Using a General Vertical Coordinate Transformation 1. Description and Testing of the Model. Journal of Geophysical Research 98, 14683–14701.

Griffies, S.M., Böning, C., Bryan, F.O., Chassignet, E.P., Gerdes, R., Hasumi, H., Hirst, A., Treguier, A.M., Webb, D., 2000. Developments in ocean climate modelling. Ocean Modelling 2, 123–192.

Haidvogel, D.B., Beckmann, A., 1999. Numerical Ocean Circulation Modeling. Imperial College Press.

Haney, R.L., 1991. On the Pressure Gradient Force over Steep Topography in Sigma Coordinate Ocean Models. J. Phys. Oceanogr. 21, 610–619.

Hewitt, H.T., Copsey, D., Culverwell, I.D., Harris, C.M., Hill, R.S.R., Keen, A.B., McLaren, A.J., Hunke, E.C., 2011. Design and implementation of the infrastructure of hadgem3: the next-generation Met Office climate modelling system. Geoscientific Model Development 4, 223–253.

Hirt, C.W., Amsden, A.A., Cook, J.L., 1974. An arbitrary Lagrangian-Eulerian computing method for all flow speeds. Journal of Computational Physics 14, 227–253.

Holt, J.T., James, I.D., 2001. An S coordinate density evolving model of the northwest European continental shelf 1, Model description and density structure. Journal of Geophysical Research 106, 14015–14034.

Hughes, C.W., de Cuevas, B.A., 2001. Why Western Boundary Currents in Realistic Oceans are Inviscid: A Link between Form Stress and Bottom Pressure Torques. Journal of Physical Oceanography 31, 2871–2885.

Janjić, Z.I., 1989. On the Pressure Gradient Force Error in - Coordinate Spectral Models. Mon. Wea. Rev. 117, 2285–2292.

Large, W., Yeager, S., 2004. Diurnal to Decadal Global Forcing For Ocean and Sea-Ice Models: The Data Sets and Flux Climatologies. NCAR Technical Note NCAR/TN-460+STR.

Leclair, M., Madec, G., 2011. z-Coordinate, an Arbitrary Lagrangian-Eulerian coordinate separating high and low frequency motions. Ocean Modelling 37, 139–152.

Lemarié, F., Kurian, J., Shchepetkin, A.F., Jeroen Molemaker, M., Colas, F., McWilliams, J.C., 2012. Are there inescapable issues prohibiting the use of terrain-following coordinates in climate models? Ocean Modelling 42, 57–79.

Madec, G., 2008. NEMO ocean engine.

Madec, G., Delecluse, P., Crépon, M., Lott, F., 1996. Large-Scale Preconditioning of Deep-Water Formation in the Northwestern Mediterranean Sea. J. Phys. Oceanogr. 26, 1393–1408.

Mellor, G.L., Hakkinen, S., Ezer, T., Patchen, R., 2002. A generalization of a sigma coordinate ocean model and an intercomparison of model vertical grids., in: Pinardi, N., Woods, J.D. (Eds.), Ocean Forecasting: Conceptual Basis and Applications.. Springer, New York, pp. 55–72.

O'Dea, E.J., Arnold, A.K., Edwards, K.P., Furner, R., Hyder, P., Martin, M.J., Siddorn, J.R., Storkey, D., While, J., Holt, J.T., Liu, H., 2012. An operational ocean forecast system incorporating NEMO and SST data assimilation for the tidally driven European North-West shelf. Journal of Operational Oceanography , 3–17.

Pacanowski, R.C., Gnanadesikan, A., 1998. Transient Response in a Z-Level Ocean Model That Resolves Topography with Partial Cells. Mon. Wea. Rev. 126, 3248–3270.

Phillips, N.A., 1957. A coordinate system having some special advantages for numerical forecasting. Journal of Meteorology 14, 184–185.

Pietrzak, J., Jakobson, J.B., Burchard, H., Jacob Vested, H., Petersen, O., 2002. A three-dimensional hydrostatic model for coastal and ocean modelling using a generalised topography following co-ordinate system. Ocean Modelling 4, 173–205.

Roberts, M.J., Wood, R.A., 1997. Topographic Sensitivity Studies with a BryanCox-Type Ocean Model. J. Phys. Oceanogr. 27, 823–836.

Schär, C., Leuenberger, D., Fuhrer, O., Lüthi, D., Girard, C., 2002. A new vertical coordinate formulation for atmospheric prediction models. Monthly Weather Review 130, 2459–2480.

Shchepetkin, A., McWilliams, J., 2005. The regional oceanic modeling system (ROMS): a split-explicit, free-surface, topography-following-coordinate oceanic model. Ocean Modelling 9, 347–404.

Shchepetkin, A.F., McWilliams, J.C., 2003. A method for computing horizontal pressure-gradient force in an oceanic model with a nonaligned vertical coordinate. Journal of Geophysical Research 108, 3090–3024.

Song, Y., Haidvogel, D.B., 1994. A semi-implicit ocean circulation model using a generalized topography-following coordinate system. Journal of Computational Physics 115, 228–244.

Song, Y.T., Hou, T.Y., 2006. Parametric vertical coordinate formulation for multiscale, Boussinesq, and non-Boussinesq ocean modeling. Ocean Modelling 11, 298–332.

Song, Y.T., Wright, D.G., 1998. A General Pressure Gradient Formulation for Ocean Models. Part II: Energy, Momentum, and Bottom Torque Consistency. Monthly Weather Review 126, 3231–3247.

Storkey, D., Blockley, E.W., Furner, R., Guiavarc'h, C., Lea, D., Martin, M.J., Barciela, R.M., Hines, A., Hyder, P., Siddorn, J.R., 2010. Forecasting the ocean state using NEMO: The new FOAM system. Journal of Operational Oceanography 3, 3–15.

Winton, M., Hallberg, R., Gnanadesikan, A., 1998. Simulation of Density-Driven Frictional Downslope Flow in Z-Coordinate Ocean Models. J. Phys. Oceanogr. 28, 2163–2174.